

Single-Site Heterogeneous Catalysts for Olefin Polymerization Enabled by Cation Exchange in a Metal-Organic Framework

Robert J. Comito,[†] Keith J. Fritzsche,[‡] Benjamin J. Sundell,[§] Klaus Schmidt-Rohr,[‡] and Mircea Dincă^{*,†}

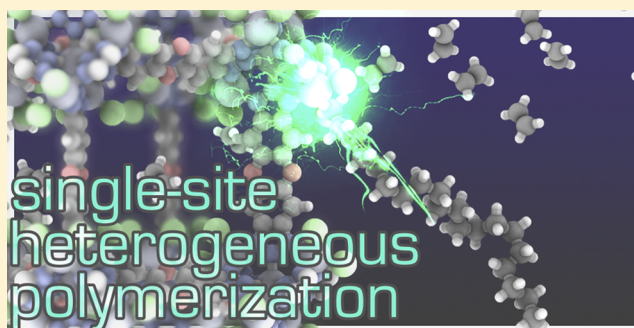
[†]Department of Chemistry, Massachusetts Institute of Technology, 77 Massachusetts Avenue, Cambridge, Massachusetts 02139, United States

[‡]Department of Chemistry, Brandeis University, 415 South St, Waltham, Massachusetts 02453, United States

[§]Aramco Research Center, Aramco Services Company, 400 Technology Square, Cambridge, Massachusetts, 02139, United States

S Supporting Information

ABSTRACT: The manufacture of advanced polyolefins has been critically enabled by the development of single-site heterogeneous catalysts. Metal-organic frameworks (MOFs) show great potential as heterogeneous catalysts that may be designed and tuned on the molecular level. In this work, exchange of zinc ions in $Zn_5Cl_4(BTDD)_3$, $H_2BTDD = \text{bis}(1H\text{-}1,2,3\text{-triazolo}[4,5\text{-}b],[4',5'\text{-}i])\text{dibenzo}[1,4]\text{dioxin}$ (MFU-4l) with reactive metals serves to establish a general platform for selective olefin polymerization in a high surface area solid promising for industrial catalysis. Characterization of polyethylene produced by these materials demonstrates both molecular and morphological control. Notably, reactivity approaches single-site catalysis, as evidenced by low polydispersity indices, and good molecular weight control. We further show that these new catalysts copolymerize ethylene and propylene. Uniform growth of the polymer around the catalyst particles provides a mechanism for controlling the polymer morphology, a relevant metric for continuous flow processes.



INTRODUCTION

The advent and development of single-site catalysts for olefin polymerization has dramatically transformed the polyolefins sector from a commodity market to a highly dynamic and specialized industry.¹ This “metallocene revolution” depended heavily on structurally tunable molecular catalysts that offer fine control over the polymer’s molecular structure. However, homogeneous catalysis remains challenging for the production of commercial polyethylene and polypropylene, whose insolubility contributes to line fouling and reactor walling under conventional solution phase reactor conditions.² Typically, industrial slurry and gas phase polymerization of ethylene and propylene rely on granular solid catalysts that are designed to provide solid polymers as free-flowing powders or beads.³

Toward this end, the commercialization of advanced ethylene and propylene polymers has focused on the development of single-site heterogeneous catalysts.⁴ However, conventional solid catalysts lack the fine electronic and steric control that underlie selectivity in homogeneous transition metal catalysts.⁵ Furthermore, multisite reactivity in solid catalysts complicates structure–activity analysis and limits control over the polymer microstructure. For these reasons, the scalable polymerization of ethylene and propylene with morphological and molecular control has largely depended on the immobilization of well-defined molecular catalysts onto suitably chosen solid supports.^{3,4,6}

In contrast, metal-organic frameworks (MOFs) offer unprecedented opportunities for structural design and tunability in the solid state through variations in both secondary building units (SBUs) and organic linkers.⁷ In catalysis, MOFs have been exploited primarily in the context of Lewis acid catalysis with SBUs or by incorporating known molecular catalysts as linkers.⁸ However, the SBUs behave as unique supramolecular ligands for transition metals, providing an intriguing platform for other types of heterogeneous catalysis.⁹ Transition metals at these nodes may be modified and substituted with preservation of the basic coordination scaffold as a result of the geometric constraints imposed by the MOF crystal lattice. Consequently, cation exchange at the SBUs offers a rational method for introducing metals of interest into a well-defined coordination environment even when analogous molecular coordination compounds are elusive or MOFs with those metals of interest are unavailable by direct synthesis.¹⁰

Among the MOFs reported to undergo cation exchange with transition metals, MFU-4l ($MFU\text{-}4l = Zn_5Cl_4(BTDD)_3$, $H_2BTDD = \text{bis}(1H\text{-}1,2,3\text{-triazolo}[4,5\text{-}b],[4',5'\text{-}i])\text{dibenzo}[1,4]\text{dioxin}$) seemed the most promising system for olefin polymerization based on the structure of the SBU.¹¹ This cluster consists of five zinc atoms: one central atom coordinated octahedrally by six nitrogens, and four peripheral

Received: May 20, 2016

Published: July 21, 2016

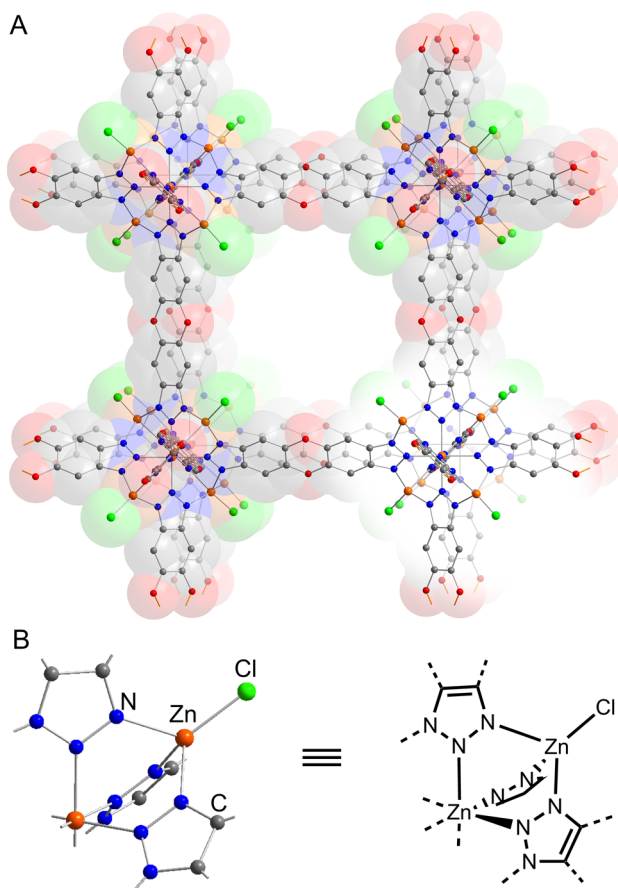


Figure 1. Portion of (A) the crystal structure of MFU-4l and (B) the structure of the SBU, illustrating the environment of the tetrahedral Zn ion replaced by Cr or Ti.

tetrahedral zinc atoms coordinated by three triazole groups and one chloride that points toward the center of the pore (Figure 1). The soft, tripodal coordination environment of the peripheral zinc ions bears structural analogy to the post-metallocene family of scorpionate ligands for ethylene polymerization.¹² Importantly, these zinc ions undergo cation exchange with late transition metals^{10d,e} and give rise to site-isolated species that engage in a variety of reactions reminiscent of scorpionate complexes. Most relevantly, we recently showed that Ni-exchanged MFU-4l is highly active and selective for the dimerization of ethylene to 1-butene, suggesting that catalysis based on alkylation and olefin insertion is possible at this

SBU.^{9d} By analogy with the molecular Cr and Ti scorpionate complexes, we reasoned that targeting Cr- and Ti-substituted MFU-4l would lead to efficient olefin polymerization catalysts.

RESULTS AND DISCUSSION

To incorporate Ti and Cr, we initially evaluated cation exchange under conditions successful for the incorporation of late transition metals into MFU-4l. However, treatment of MFU-4l with the more oxophilic and generally more air-sensitive titanium and chromium halides was unsuccessful at elevated temperature, leading to decomposition of the MOF or the metal precursors. The exchanges were successful, however, at room temperature, where various amounts of Cr²⁺, Cr³⁺, Ti³⁺, or Ti⁴⁺ readily exchanged zinc ions in MFU-4l, as determined by inductively coupled plasma atomic emission spectroscopy (ICP-AES, Table 1). Thus, soaking solid MFU-4l in a DMF solution with excess CrCl₃(THF)₂(H₂O) and catalytic Cr²⁺ replaces all four exchangeable Zn sites in every SBU to give a material with the composition (Cr^{III}Cl₂)₄Zn-(BTDD)₃. On the other hand, exchange with just CrCl₂ replaces only approximately two zinc atoms per SBU under similar conditions. Successful exchange with titanium chlorides required switching the solvent to acetonitrile; treatment of MFU-4l with excess TiCl₃(THF)₃ leads to substitution of nearly 2 equiv of Zn per SBU, while only ~0.2 Zn atoms per SBU are displaced when excess TiCl₄(THF)₂ is used. Notably the loading may be controlled by tuning the excess of transition metal used for the exchange, and two samples of Cr-exchanged MFU-4l with lower loading were prepared for comparison.

Powder X-ray diffraction (PXRD) patterns agree well with that of the parent material, demonstrating that the lattice structure of the MOF has been preserved (Figures S3.1 and S3.2). Furthermore, N₂ adsorption analyses indicate high saturation loadings and Brunauer–Emmet–Teller apparent surface areas that compare favorably with the parent material (Figure S3.5). Taken together with the detection of zinc in the exchange supernatant, also determined by ICP-AES, these results are consistent with incorporation of chromium and titanium into the SBU by cation exchange. In addition, the CrCl₂- and TiCl₃-exchanged materials are expectedly sensitive when exposed to air and undergo visible color changes, whereas the CrCl₃- and TiCl₄-exchanged samples do not, suggesting conservation of the transition metal's oxidation state upon cation exchange. The differences observed in loading efficiency and in catalytic activity between samples exchanged with the

Table 1. Exchange of Early Transition Metals in MFU-4l

entry	MOF	Zn ₅ Cl ₄ (BTDD) ₃ (MFU-4l) $\xrightarrow[23^\circ\text{C}, 7-8 \text{ days}]{\text{MCl}_x \text{ solvent}}$ M _y Zn _{5-y} (BTDD) ₃		BET area ^b
		MCl _x solvent	M:Zn ^a	
1	Ti(III)-MFU-4l	TiCl ₃ (THF) ₃ , CH ₃ CN	1.6:3.4	3144 ± 11
2	Ti(IV)-MFU-4l	TiCl ₄ (THF) ₂ , CH ₃ CN	0.2:4.8	3934 ± 15
3	Cr(II)-MFU-4l	CrCl ₂ , DMF	2.4:2.6	4060 ± 27
4	Cr(III)-MFU-4l	CrCl ₃ (THF) ₂ (H ₂ O), CrCl ₂ , ^c DMF	4.0:1.0	3665 ± 18
5	Cr(II)-MFU-4l (low loading)	CrCl ₂ , CH ₃ OH	0.35:4.65	4329 ± 12
6	Cr(III)-MFU-4l (low loading)	CrCl ₃ (THF) ₂ (H ₂ O), CrCl ₂ , ^c DMF	0.25:4.75	3429 ± 40
7	MFU-4l			4114 ± 15

^aMetal ratios determined by ICP-AES or ICP-MS. ^bApparent BET surface areas determined by N₂ adsorption analysis at 77 K (cm³/mmol). ^cIn catalytic quantities.

Table 2. Catalytic Polymerization of Ethylene by Cr- and Ti-MOFs and Characterization of the Resulting Polymers

entry	precatalyst	activator ^a	P (ethylene)	P (H ₂)	TOF ^b	X _C ^c	T _M ^c	M _w (×10 ⁶) ^d	M _N (×10 ⁶) ^d	PDI ^d
1	Ti(III)-MFU-4l	AlEt ₃	40 bar	0 bar	11 000	58%	138 °C	1.2	0.4	2.9
2	Ti(III)-MFU-4l	MAO	40 bar	0 bar	15 000	58%	135 °C	1.0	0.3	3
3	Ti(IV)-MFU-4l	AlEt ₃	40 bar	0 bar	1330	50%	136 °C	1.2	0.6	2.0
4	Ti(IV)-MFU-4l	MAO	40 bar	0 bar	1860	50%	135 °C	1.1	0.6	2.0
5	Cr(III)-MFU-4l	AlEt ₃	40 bar	0 bar	5100	67%	135 °C	0.7	0.2	4
6	Cr(III)-MFU-4l	MAO	40 bar	0 bar	3420	66%	133 °C	0.5	0.1	5
7	Cr(II)-MFU-4l	MAO	40 bar	0 bar	4770	60%	134 °C	0.7	0.1	7
8	Cr(III)-MFU-4l (low)	AlEt ₃	40 bar	0 bar	7300	66%	131 °C			
9	Cr(III)-MFU-4l (low)	MMAO-12	40 bar	0 bar	7200	67%	131 °C			
10	Cr(II)-MFU-4l (low)	MMAO-12	40 bar	0 bar	7800	63%	134 °C			
11	Ti(III)-MFU-4l	MAO	9 bar	0 bar	2850	56%	135 °C	1.4	0.6	2.3
12	Ti(III)-MFU-4l	MAO	5 bar	0 bar	1750	54%	135 °C	1.3	0.7	1.8
13	Ti(III)-MFU-4l	MAO	13 bar	2 bar	3380	67%	138 °C	0.5	0.08	6
14	Ti(III)-MFU-4l	MAO	10 bar	10 bar	1620	77%	135 °C	0.2	0.04	7

^aFor loading, see the Supporting Information. ^bTurnover frequency (TOF) = moles of ethylene consumed per mole exchanged metal per hour. ^cSecond scan percent crystallinity (X_C) and melting peak (T_M) evaluated by differential scanning calorimetry. ^dWeight-average molecular weight (M_w), number-average molecular weight (M_N), and polydispersity index (PDI) determined by high-temperature gel permeation chromatography.

same metal in different oxidation states also suggest oxidation state conservation (see below).

Notably, all attempts to prepare MOFs analogous to MFU-4l with chromium or titanium by direct solvothermal synthesis failed. Combining H₂BTDD with chromium and titanium salts under air-free conditions yielded amorphous materials or unidentified mixed crystalline phases according to PXRD analysis performed under inert atmosphere. This result is unsurprising given the relative paucity of azolate MOFs based on oxophilic titanium and chromium,¹³ and underscores the versatility of cation exchange for accessing metastable phases.

With MOF samples suitably loaded with early transition metals, we sought to explore their effectiveness in heterogeneous olefin polymerization. When treated with methylaluminoxane (MAO) or triethylaluminum in toluene and then pressurized with ethylene, all four samples polymerize ethylene catalytically, with activities ranging between 1300 and 15 000 turnovers per hour at 40 bar of ethylene (Table 2). In contrast, no observable ethylene oligomerization or polymerization products were detected with the all-zinc precursor MFU-4l and MAO under similar conditions. We therefore attribute the catalytic activity to the exchanged transition metals.

The polymers produced by all four catalysts were identified as high or ultrahigh molecular weight, high-density polyethylene (HDPE)¹⁴ using a variety of molecular characterization techniques. Crystallinity and peak melting temperature were evaluated by differential scanning calorimetry (DSC) using a standard two-scan method for thermally resetting the polymers in order to avoid inconsistencies in the thermal and mechanical history of samples.¹⁵ All polymeric products displayed high crystallinity (50–65%) and melting temperatures (133–138 °C), characteristic of HDPE. Magic angle spinning ¹³C NMR spectra of samples 2, 4, and 6 in Table 2 showed large sharp crystal peaks (at 32.8 and 34.2 ppm) and a broader shoulder at 32 ppm that can be attributed to methylenes in the orthorhombic and monoclinic crystallites

and the amorphous regions, respectively (Figures 2A and S8.2).¹⁶ Notably, a small peak at 15 ppm can be assigned to methyl groups of chain-ends or terminating long-chain branches. The polymers were further analyzed by high-temperature gel permeation chromatography (HT-GPC). This technique indicated apparent number-averaged molecular weights (M_N) ranging from 0.1 × 10⁶ for the polymer produced by Cr(III)-MFU-4l to 0.6 × 10⁶ for the polymer produced by Ti(IV)-MFU-4l. These data show that the titanium catalysts consistently produce polymers of higher molecular weight than the chromium catalysts, a conclusion consistent with the generally lower second-scan crystallinities obtained for the titanium-produced polymers, as evaluated by DSC. When comparing the chromium catalysts at high and at low loading, roughly similar thermal parameters are obtained for polymers obtained with the same activator and exchange cation (entries 5–10). However, a higher activity is observed at lower loading.

Notably, the polydispersity indices derived by HT-GPC are generally low, ranging from 5 for Cr(III)-MFU-4l to 2.0 for Ti(IV)-MFU-4l at 40 bar of ethylene. These PDI values are considerably lower than those reported for polyethylene produced from molecular scorpionate complexes of titanium and chromium.¹⁸ The low polydispersities further suggest single-site polymerization activity, which has not been previously demonstrated in a MOF.¹⁹

Comparison of the number-averaged molecular weights calculated assuming linear chains from NMR and HT-GPC, see Table S8.1, suggests the presence of about 10 long branches per polymer main chain. Such long-chain branching, which is desirable for easier polymer processability,²⁰ causes the radius of gyration to contract, compared to a linear chain of the same M_N; therefore, the true M_N would be larger than the values obtained by HT-GPC.²¹ We also note that HT-GPC data is notoriously sensitive to the method of analysis. For an alternative analysis, with qualitatively similar trends, see Table S6.1.

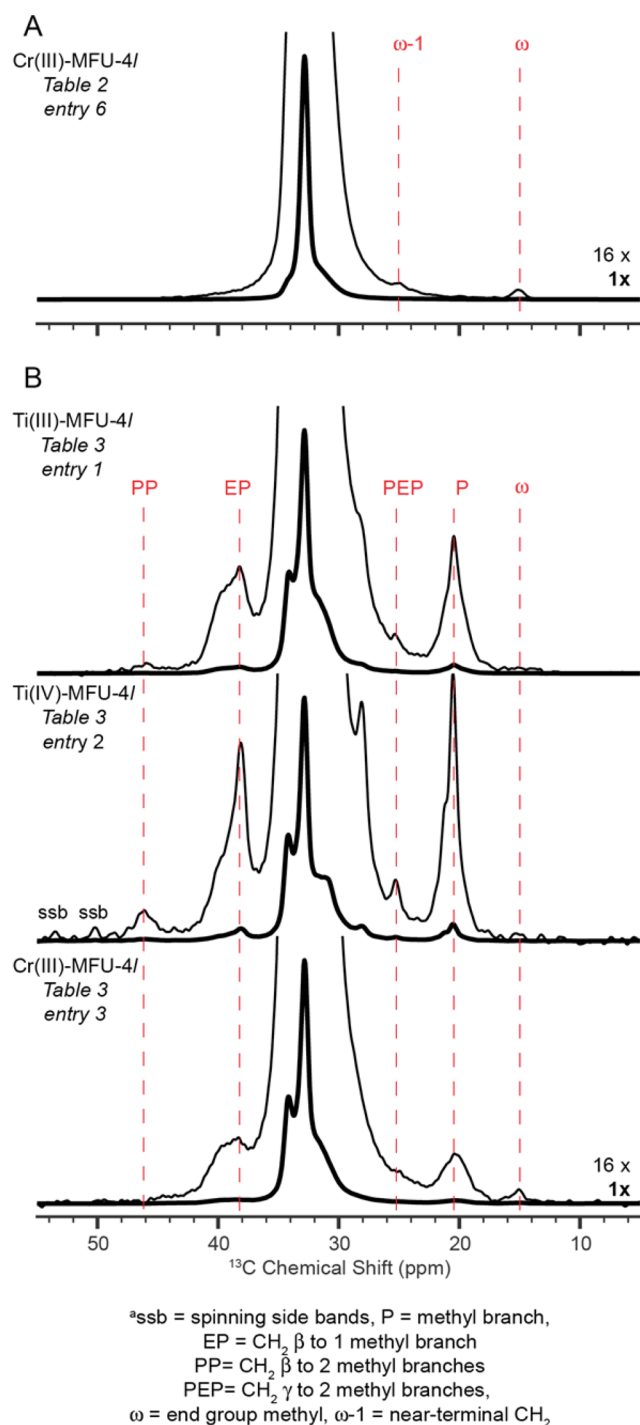


Figure 2. Quantitative multiCP¹⁷/MAS ¹³C NMR spectra of (A) an ethylene homopolymer and (B) ethylene-propylene copolymers (magic angle spinning frequency: 4.5 kHz).

To explore the molecular selectivity afforded by our catalysts, we investigated the product of the most active analogue, Ti(III)-MFU-4l, as a function of ethylene pressure. The TOF of Ti(III)-MFU-4l decreases proportionally with pressure, and is accompanied by a concomitant increase of M_N for the resulting polymers (Table 2, entries 2, 8, and 9).²² This pressure dependence suggests that polymerization occurs by the Cossee-Arlman mechanism involving direct chain transfer to monomer.²³ Consequently, the decrease of PDI with decreasing pressure can be explained by ethylene concentration

Table 3. Copolymerization of Ethylene and Propylene

entry	precatalyst	TOF ^a	X_C^b	T_M^b	% propylene ^c
1	Ti(III)-MFU-4l	3806	37%	125 °C	4 ± 1%
2	Ti(IV)-MFU-4l	126	38%	127 °C	6.7 ± 1.3%
3	Cr(III)-MFU-4l	95	54%	128 °C	2 ± 0.5%

^aReported as moles of ethylene consumed per mole of exchanged metal per hour. ^bEvaluated by double-scan DSC. ^cDetermined by solid-state NMR.

gradients during catalysis.²⁴ Because the molecular weight depends on pressure, variation in the local ethylene concentration would be expected to increase the polydispersity. Conversely, at reduced pressure a slower consumption of ethylene would mitigate concentration gradients, consistent with a decrease in PDI.

Industrially, controlling polymer molecular weight through coloading with hydrogen is a highly desired mode of molecular control. Typically, single-site catalysts offer better molecular control than multisite catalysts, which suffer from varying response to hydrogen at distinct catalyst sites.¹ Consistently, treatment of Ti(III)-MFU-4l with an increasing ratio of hydrogen to ethylene leads to a decrease in molecular weight (Table 2, entries 2, 10, and 11). As the hydrogen:ethylene ratio increases and reaches 1:1, the crystallinity determined by DSC also increases from 58% to 77%, while M_N decreases nearly 10-fold.

Likewise, the incorporation of comonomers provides one of the most general means for tuning the properties of polyolefins, and single-site catalysts offer numerous advantages over multisite catalysts for copolymerization. Toward this end, we evaluated the copolymerization of ethylene and propylene under conditions similar to our homopolymerization studies (Table 3). In all cases, the products could be characterized as copolymers. DSC analysis indicated a significant reduction in both crystallinity and peak melting temperatures relative to the homopolymers produced by the same catalyst, consistent with side chain branching. Infrared spectra of the resulting copolymers display a sharp peak at 1378–1379 cm⁻¹, consistent with the characteristic C–CH₃ stretch observed for methyl-branched polyethylene (Figures S6.39–S6.41), whereas homopolymers exhibit IR spectra consistent with linear or minimally branched polyethylene.²⁵

In order to confirm our molecular assignments and to quantify propylene incorporation, the copolymers were also analyzed by quantitative ¹³C MultiCP/MAS NMR.²⁶ Three copolymers produced by Ti(III)-, Ti(IV)- and Cr(III)-MFU-4l were chosen for analysis and compared with the homopolymers produced by the same precatalysts (Figure 2B). In addition to the peaks seen in the homopolymers, the copolymer spectra exhibit clear methyl and methine signals at 20 and 38 ppm, respectively, characteristic of methyl branching.²⁷ Quantification of propylene incorporation demonstrates considerable differences in copolymerization efficiency among the three

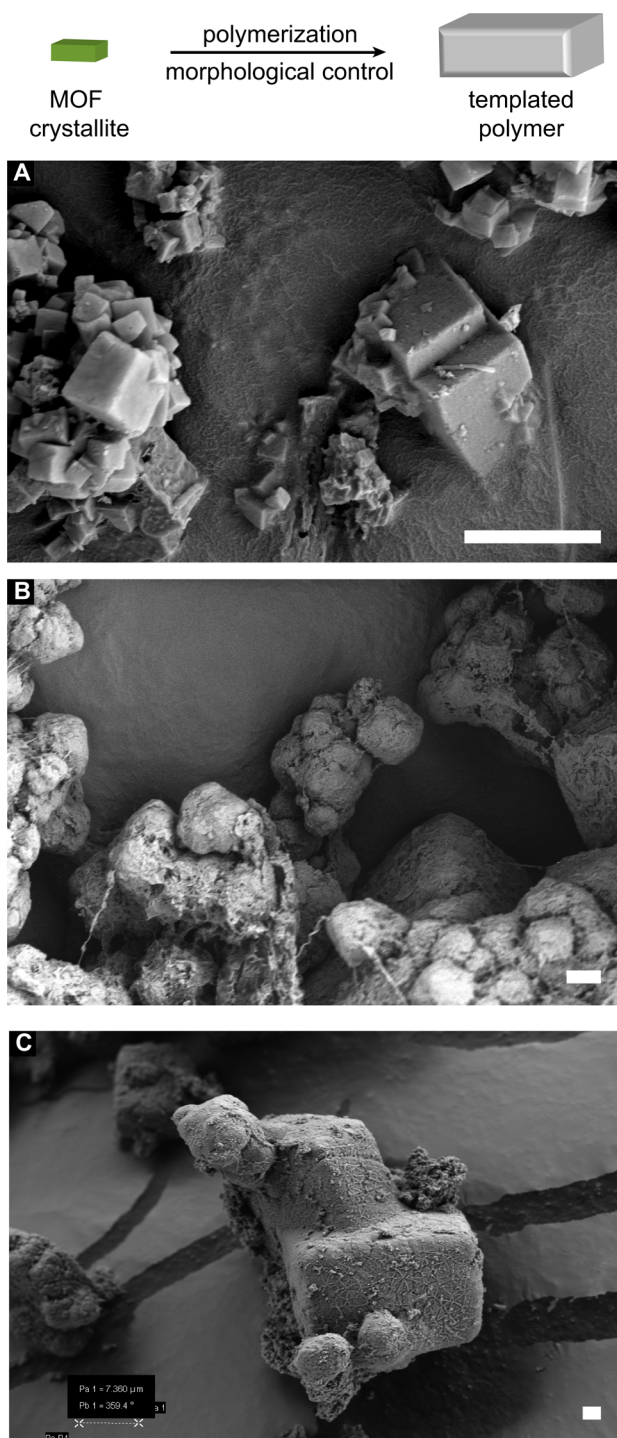


Figure 3. Scanning electron micrographs of (A) Ti(III)-MFU-4l, (B) homopolymer produced by Ti(III)-MFU-4l (Table 2, entry 2), and (C) homopolymer produced by Cr(III)-MFU-4l (Table 2, entry 6). White scale bars indicate 2 μm .

catalysts, with propylene incorporation ranging between 2 and 6.7 mol %, see Table 3. The branch contents of the copolymers produced with titanium catalysts are higher than those of the copolymer produced by Cr(III)-MFU-4l. Correspondingly, lower crystallinities and melting temperatures are observed for the copolymers produced by the titanium catalysts than for the copolymers produced by Cr(III)-MFU-4l. The peak at 46 ppm in the NMR spectra of the polymers from the two Ti-catalysts, resulting from two consecutive propylene insertions,

is ~ 10 times larger than expected for a random copolymer; nevertheless, neighboring propylene units are far less likely than ethylene-propylene pairs, which resonate near 38 ppm.²⁷

Finally, in view of the importance of polymer morphology for industrial processing, we sought to investigate the morphological control offered by our catalysts, and analyzed the resulting polymers by scanning electron microscopy (SEM). Comparison of MFU-4l and the precatalysts shows that both consist of prismatic crystallites ranging in size from 0.1–2 μm , which do not change during cation exchange (Figures 3 and S7.1–S7.8). As in industrial slurry-phase polymerization conditions, the resulting products are typically obtained as free-flowing powders with negligible solubility in common solvents at room temperature. SEM analysis of these powders demonstrated a crystallite-like shape reminiscent of the precatalyst particles, although larger in size, with some reaching 10 μm (Figures 3 and S7.10–S7.25). Qualitatively, the rounded edges and rougher surfaces observed for the polymer particles contrasts with the sharp edges and flat faces of the precatalyst crystallites. Furthermore, comparison of the polymer particles and precatalyst crystallites by SEM-EDS (energy-dispersive X-ray spectroscopy) confirmed that these cuboidal structures are polymer particles and not residual MOF: whereas SEM-EDS spectra of MOF particles exhibit significant peaks for Cr/Ti, Zn, and Cl, these peaks are nearly absent in the corresponding spectra of the polymer particles (Figures S7.9, S7.14, S7.18, and S7.22). These results are consistent with even growth of the insoluble polymer product around a granular catalyst particle, a mechanism of morphological control highly desired for industrial production of insoluble polyolefins.^{2,3}

In summary, we report four novel chromium- and titanium-containing MOFs prepared by cation exchange that are highly active for the polymerization of ethylene. These MOFs produce high molecular weight, high-density polyethylene, demonstrating features of single-site catalysis as well as morphological control over the polymer product. Furthermore, the successful copolymerization with propylene opens the door to a range of commercially significant polyolefin copolymers. Likewise, combined GPC and solid-state NMR analysis provides evidence for long-chain branching, a structural feature desirable for improving the melt viscosity of polyethylene. Efforts are underway in our laboratory to expand upon this strategy to target commercially relevant polymers and complex molecular architectures using selective heterogeneous catalysis in MOFs.

■ ASSOCIATED CONTENT

📄 Supporting Information

The Supporting Information is available free of charge on the ACS Publications website at DOI: 10.1021/jacs.6b05200.

PXRD spectra, IR spectra, N₂ adsorption isotherms, experimental details, HT-GPC chromatograms, DSC data, and NMR data (PDF)

■ AUTHOR INFORMATION

Corresponding Author

*mdinca@mit.edu

Notes

The authors declare no competing financial interest.

■ ACKNOWLEDGMENTS

This research was supported through a Research Agreement with Saudi Aramco, a Founding Member of the MIT Energy

Initiative. Fundamental studies of cation exchange in MOFs are supported by a CAREER award to M.D. from the National Science Foundation (DMR-1452612). M.D. acknowledges the Sloan Foundation, the Research Corporation for Science Advancement (Cottrell Award), and 3M for nontenured faculty funds. The authors have filed a patent on work disclosed in this Article. We thank Dr. Christopher Hendon for the production of the TOC graphic.

REFERENCES

- (1) (a) Chum, S. P.; Kao, C. I.; Knight, G. W. Structure, Properties and Preparation of Polyolefins Produced by Single-site Catalyst Technology. In *Metallocene-Based Polyolefins*; Scheirs, J., Kaminsky, W., Eds.; John Wiley & Sons Ltd.: New York, 2000; Vol. 1, p 261. (b) Heurtefeu, B.; Cramail, H.; Vaultier, F.; Boisson, C.; Leino, R. Single Site Catalysts. In *Encyclopedia of Polymer Science and Technology*, 4th ed.; Mark, H. F., Ed.; John Wiley & Sons, Inc.: Hoboken, NJ, 2014; Vol. 12, p 551.
- (2) (a) Jenny, C.; Maddox, P. *Curr. Opin. Solid State Mater. Sci.* **1998**, *3*, 94. (b) Abbenhuis, H. C. L. *Angew. Chem., Int. Ed.* **1999**, *38*, 1058. (c) Chien, J. C. W. *Top. Catal.* **1999**, *7*, 23.
- (3) (a) Severn, J. R.; Chadwick, J. C.; Duchateau, R.; Friederichs, N. *Chem. Rev.* **2005**, *105*, 4073. (b) Knuutila, H.; Lehtinen, A.; Nummila-Pakarinen, A. *Adv. Polym. Sci.* **2004**, *169*, 13.
- (4) (a) Hlatky, G. G. *Chem. Rev.* **2000**, *100*, 1347. (b) Kim, S. H.; Somorjai, G. A. *Proc. Natl. Acad. Sci. U. S. A.* **2006**, *103*, 15289. (c) Choi, Y.; Soares, J. B. P. *Can. J. Chem. Eng.* **2012**, *90*, 646.
- (5) (a) Groppo, E.; Lamberti, C.; Bordiga, S.; Spoto, G.; Zecchina, A. *Chem. Rev.* **2005**, *105*, 115. (b) McDaniel, M. P. A Review of the Phillips Supported Chromium Catalyst and Its Commercial Use for Ethylene Polymerization. In *Advances in Catalysis*; Gates, B. C., Knotzinger, H., Eds.; Elsevier: Boston, 2010; Vol. 53; p 123.
- (6) (a) Kaminsky, W.; Winkelbach, H. *Top. Catal.* **1999**, *7*, 61. (b) Kristen, M. O. *Top. Catal.* **1999**, *7*, 89.
- (7) (a) Furukawa, H.; Cordova, K. E.; O'Keefe, M.; Yaghi, O. M. *Science* **2013**, *341*, 1230444. (b) Janiak, C.; Vieth, J. K. *New J. Chem.* **2010**, *34*, 2366. (c) Zhou, H.-C.; Long, J. R.; Yaghi, O. M. *Chem. Rev.* **2012**, *112*, 673. (d) Jiang, J.; Zhao, Y.; Yaghi, O. M. *J. Am. Chem. Soc.* **2016**, *138*, 3255. (e) Zhou, H.-C.; Kitagawa, S. *Chem. Soc. Rev.* **2014**, *43*, 5415.
- (8) (a) Chughtai, A. H.; Ahmad, N.; Younus, H. H.; Laypkov, A.; Verpoort, F. *Chem. Soc. Rev.* **2015**, *44*, 6804. (b) *Metal Organic Frameworks as Heterogeneous Catalysts*; Llabrés i Xamena, F. X., Gascon, J., Eds.; The Royal Society of Chemistry: Cambridge, UK, 2013. (c) Gascon, J.; Corma, A.; Kapteijn, F.; Llabrés i Xamena, F. X. *ACS Catal.* **2014**, *4*, 361.
- (9) (a) Phan, A.; Czaja, A.; Gandara, F.; Knobler, C.; Yaghi, O. *Inorg. Chem.* **2011**, *50*, 7388. (b) Xiao, D. J.; Bloch, E. D.; Mason, J. A.; Queen, W. L.; Hudson, M. R.; Planas, N.; Borycz, J.; Dzuba, A. L.; Verma, P.; Lee, K.; Bonino, F.; Crocella, V.; Yano, J.; Bordiga, S.; Truhlar, D. G.; Gagliardi, L.; Brown, C. M.; Long, J. R. *Nat. Chem.* **2014**, *6*, 590. (c) Mondloch, J. E.; Katz, M. J.; Isley, W. C., III; Ghosh, P.; Liao, P.; Bury, W.; Wagner, G. W.; Hall, M. G.; DeCoste, J. B.; Peterson, G. W.; Snurr, R. Q.; Cramer, C. J.; Hupp, J. T.; Farha, O. K. *Nat. Mater.* **2015**, *14*, 512. (d) Metzger, E. D.; Brozek, C. K.; Comito, R. J.; Dincă, M. *ACS Cent. Sci.* **2016**, *2*, 148.
- (10) (a) Kim, Y.; Das, S.; Bhattacharya, S.; Hong, S.; Kim, M. G.; Yoon, M.; Natarajan, S.; Kim, K. *Chem. - Eur. J.* **2012**, *18*, 16642. (b) Lalonde, M.; Bury, W.; Karagiari, O.; Brown, Z.; Hupp, J. T.; Farha, O. K. *J. Mater. Chem. A* **2013**, *1*, 5453. (c) Brozek, C. K.; Dincă, M. *Chem. Soc. Rev.* **2014**, *43*, 5456. (d) Denysenko, D.; Werner, T.; Grzywa, M.; Puls, A.; Hagen, V.; Eickerling, G.; Jelic, J.; Reuter, K.; Volkmer, D. *Chem. Commun.* **2012**, *48*, 1236. (e) Brozek, C. K.; Bellarosa, L.; Soejima, T.; Clark, T. V.; Lopez, N.; Dincă, M. *Chem. - Eur. J.* **2014**, *20*, 6871.
- (11) Denysenko, D.; Grzywa, M.; Tonigold, M.; Streppel, B.; Krkljus, I.; Hirscher, M.; Mugnaioli, E.; Kolb, U.; Hanss, J.; Volkmer, D. *Chem. - Eur. J.* **2011**, *17*, 1837.
- (12) (a) Baier, M. C.; Zuideveld, M. A.; Mecking, S. *Angew. Chem., Int. Ed.* **2014**, *53*, 9722. (b) Domsjki, G. J.; Rose, J. M.; Coates, G. W.; Bolig, A. D.; Brookhart, M. *Prog. Polym. Sci.* **2007**, *32*, 30. (c) Garcia-Orozco, I.; Quijada, R.; Vera, K.; Valderrama, M. *J. Mol. Catal. A: Chem.* **2006**, *260*, 70. (d) Denysenko, D.; Grzywa, M.; Jelic, J.; Reuter, K.; Volkmer, D. *Angew. Chem., Int. Ed.* **2014**, *53*, 5832.
- (13) Kongpatpanich, K.; Horike, S.; Sugimoto, M.; Fukushima, T.; Umeyama, D.; Tsutsumi, Y.; Kitagawa, S. *Inorg. Chem.* **2014**, *53*, 9870.
- (14) High-density polyethylene is defined as having a density range of 0.94–0.97 g/mL. Peacock, A. J. *Handbook of Polyethylene; Structure, Properties, and Applications*; Marcel Dekker, Inc.: New York, 2000.
- (15) Mark, J. E. *Physical Properties of Polymers Handbook*; AIP: Woodbury, NY, 1996.
- (16) VanderHart, D. L.; Khoury, F. *Polymer* **1984**, *84*, 90151.
- (17) Johnson, R. L.; Schmidt-Rohr, K. *J. Magn. Reson.* **2014**, *239*, 44.
- (18) (a) Rojas, R.; Valderrama, M.; Wu, G. *Inorg. Chem. Commun.* **2004**, *7*, 1295. (b) Murtuza, S.; Casagrande, O. L.; Jordan, R. F. *Organometallics* **2002**, *21*, 1882.
- (19) Ethylene polymerization by MOFs has recently been reported by a number of groups. In one report, molecular weight distributions clearly implicate multisite reactivity Li, H.; Xu, B.; He, J.; Liu, X.; Gao, W.; Mu, Y. *Chem. Commun.* **2015**, *51*, 16703. In another recent report, the product's molecular weight distribution was not reported Klet, R. C.; Tussupbayev, S.; Borycz, J.; Gallagher, J. R.; Stalzer, M. M.; Miller, J. T.; Gagliardi, L.; Hupp, J. T.; Marks, T. J.; Cramer, C. J.; Delferro, M.; Farha, O. K. *J. Am. Chem. Soc.* **2015**, *137*, 15680.
- (20) Gahleitner, M. *Prog. Polym. Sci.* **2001**, *26*, 895.
- (21) Zimm, B. H.; Stockmayer, W. H. *J. Chem. Phys.* **1949**, *17*, 1301.
- (22) A similar chain selectivity trend was observed with the Ni-MFU-4l-catalyzed dimerization of ethylene to 1-butene under similar conditions, whereby an increasing yield of higher olefins (1-hexene, 1-octene) selectivity was observed as the pressure was decreased (ref 9d).
- (23) (a) Resconi, L.; Cavallo, L.; Fait, A.; Piemontesi, F. *Chem. Rev.* **2000**, *100*, 1253. (b) Margl, P.; Deng, L.; Ziegler, T. *J. Am. Chem. Soc.* **1999**, *121*, 154.
- (24) Böhm, L. L. *Angew. Chem., Int. Ed.* **2003**, *42*, 5010.
- (25) Nishikida, K.; Coates, J. Infrared and Raman Analysis of Polymers. In *Handbook of Plastics Analysis*; Lobo, H., Bonilla, J. V., Eds.; Marcel Dekker Inc.: New York, 2003.
- (26) Solution-phase characterization of polyethylenes by ¹³C NMR has been reported. However, our products had limited solubility in relevant NMR solvents even at temperatures exceeding 120 °C, consistent with the high molecular weight determined by gel permeation chromatography. (a) Galland, G. B.; de Souza, R. F.; Mauler, R. S.; Nuñez, F. F. *Macromolecules* **1999**, *32*, 1620. (b) Zhou, Z.; Kümmerle, R.; Stevens, J. C.; Redwine, D.; He, Y.; Qiu, X.; Cong, R.; Klosin, J.; Montañez, N.; Roof, G. *J. Magn. Reson.* **2009**, *200*, 328. (c) Lee, K.-B.; Kweon, J.; Lee, H.-J.; Park, H. *Polym. J.* **1996**, *28*, 696. (d) Cuomo, C.; Milione, S.; Grassi, A. *Macromol. Rapid Commun.* **2006**, *27*, 611. (e) Usami, T.; Takayama, S. *Macromolecules* **1984**, *17*, 1756.
- (27) Grant, D. M.; Paul, E. G. *J. Am. Chem. Soc.* **1964**, *86*, 2984.